

## Precision Measurements of Low Energy Positron Fluxes by AMS

---

**C. Gámez<sup>a,\*</sup> and J. Casaus, M. A. Velasco<sup>a</sup>**

<sup>a</sup>*Centro de Investigaciones Energéticas, Medioambientales y Tecnológicas (CIEMAT),  
Avda. Complutense 40, Madrid, Spain*

*E-mail:* [carmen.gamez@ciemat.es](mailto:carmen.gamez@ciemat.es)

The detailed measurement of daily cosmic positron fluxes in the energy interval from 1.00 to 41.9 GeV based on the data collected with the Alpha Magnetic Spectrometer (AMS) aboard the International Space Station from May 2011 to May 2021 will be discussed. The analysis shows time variations at different time scales associated with solar activity over half of the solar cycle 24 and the beginning of the 25. The time evolution of cosmic rays of opposite charge signs and different masses are simultaneously measured, covering the reversal of the Sun's magnetic field polarity, allowing to compare the different positron fluxes variations from the electron and proton fluxes at short and long time scales.

*41st International Conference on High Energy physics - ICHEP2022  
6-13 July, 2022  
Bologna, Italy*

---

\*Speaker

## 1. Introduction: Cosmic Rays in the Heliosphere

To reach the Earth, cosmic rays must penetrate the Heliosphere of the Solar System, a region in the Local Interstellar Medium where the solar activity dominates the environment. In consequence, the cosmic rays measured near the Earth are significantly affected by the solar activity or solar modulation. The solar activity follows an 11-year cycle during which the configuration of the coronal solar magnetic lines changes due to the reversal of the solar dipole magnetic field. Since the solar modulation depends on the charge-sign of the particles, a complete understanding of the solar modulation requires accurate measurements of particles with different charge signs.

## 2. The AMS-02 Detector

AMS-02 is a multipurpose particle physics detector designed to carry out accurate measurements of cosmic ray charged particles in the GeV-TeV range. It was installed on 19 May 2011 aboard the International Space Station (ISS) and has continuously taken data since its installation. After more than 11 years of operation on the ISS, AMS-02 has collected more than  $2 \times 10^{11}$  cosmic rays events in a long-term mission that will continue during the ISS lifetime until 2030.

The detector consists of 6 different sub-detectors that measure the charge ( $Z$ ), energy ( $E$ ), mass ( $m$ ), momentum ( $p$ ) or rigidity ( $R = p/Z$ ) and velocity ( $\beta = v/c$ ) independently: nine layers of precision Silicon Tracker (STD) with an inner tracker (L2-L8) inside a permanent magnet and two outer layers (L1 and L9), one at the top and the other at the bottom of the detector; a Transition Radiation Detector (TRD); four planes of Time Of Flight counters (TOF); a Ring Imaging Cherenkov detector (RICH); an array of anti-coincidence counters (ACC) surrounding the inner tracker; and an Electromagnetic Calorimeter (ECAL). More details on the sub-detectors can be found in [1, 2].

## 3. Positron identification

The two key detectors for positron identification are the ECAL and the TRD. These sub-detectors allow the rejection of the overwhelming background coming mainly by protons.

- **TRD:** The signals observed in all TRD layers associated with the incoming particle are combined in a log-likelihood estimator  $\Lambda_{TRD}$  formed from the ratio of the log-likelihood probability of the  $e^\pm$  hypothesis to that of the proton hypothesis. The distinctly different  $\Lambda_{TRD}$  distributions for  $e^{+/-}$  and protons allows an efficient discrimination between the positron signal and the proton background. The achieved proton rejection is shown in Figure 1a. As seen, the TRD provides a proton rejection above  $10^3$  up to 200 GeV for a 90% efficiency in the positron signal.
- **ECAL:** The  $e^\pm$  are identified from the proton background by means of a statistical estimator which exploits the different characteristics of the electromagnetic and hadronic showers. The estimator combines 16 variables from the imaging reconstruction of the electromagnetic shower. The proton rejection power, which combines the ECAL estimator with the energy-momentum matching ( $E/p > 0.7$ ) is shown in figure 1b evaluated as a function of energy. As seen, the ECAL, together with the consistency between  $E$  and  $p$  measurements, provides a proton rejection above  $10^4$  up to 700 GeV with 90% efficiency in the positron signal.

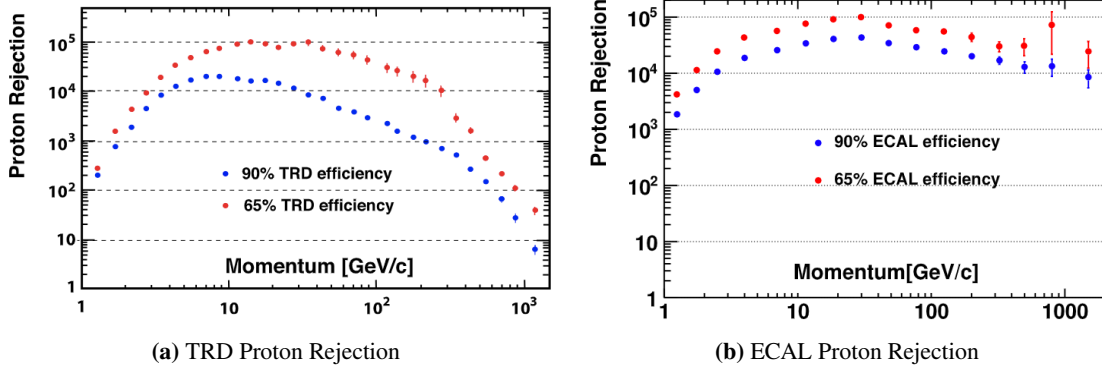


**Figure 1:** (a) Proton rejection power of the TRD at 90% and 65% electron and positron efficiency. At 90%  $e^\pm$  efficiency, the measured proton rejection is above  $10^3$  up to 200 GeV. At higher energies, the rejection power can be improved by tightening the  $e^\pm$  selection. (b) Comparison of the measured proton rejection for 90% (blue data points) and 65% (red data points)  $e^\pm$  selection efficiencies. The tighter cut in the ECAL estimator further reduces the proton background by a factor of  $\sim 3$  [2].

#### 4. Daily Positron Flux

In this analysis, the selected events are required to be downward going particles with a relativistic velocity  $\beta > 0.8$  measured by the four TOF planes, charge reconstructed by the TOF and tracker compatible with  $Z = 1$ , to have a reconstructed shower in the ECAL and a reconstructed track in the TRD and in the tracker. In addition, track fitting quality criteria, as  $\chi^2 < 20$ , both in the bending and non-bending planes are applied to ensure the accuracy of the track reconstruction. In order to select primary cosmic rays, the measured energy in the ECAL is required to be greater than the maximum local geomagnetic cutoff [3]. After the selection and background subtraction (see section 3), the daily positron flux is calculated following the equation 1<sup>1</sup>

$$\phi_i^j = \frac{N_i^j}{A_i^j (1 + \delta_i^j) \epsilon_i^j T_i^j \Delta E_i} \quad (1)$$

where  $N_i^j$  is the number of positrons,  $A_i^j$  is the effective acceptance calculated from the Monte Carlo simulation,  $\delta_i^j$  is the small correction to the acceptance estimated by comparing the efficiencies in data and MC simulation,  $\epsilon_i^j$  is the trigger efficiency, and  $T_i^j$  is the data collection time.

The precise measurements of daily cosmic positron flux in the energy interval from 1.00 to 11.00 GeV collected by AMS-02 aboard the International Space Station from May 2011 to May 2021 is shown in figure 2. These measurements cover part of the solar cycle 24 and the beginning of solar cycle 25, and the shaded area corresponds to the time period when the solar magnetic field polarity reversed. As seen, the positron flux exhibits variations at different timescales; short-term variations (on the scale of days and months) and long-term variations (on the scale of years). These variations decrease with increasing energy.

<sup>1</sup>Equation for daily isotropic flux in the  $i$ th energy bin ( $E_i, E_i + \Delta E_i$ ) and  $j$ th day.

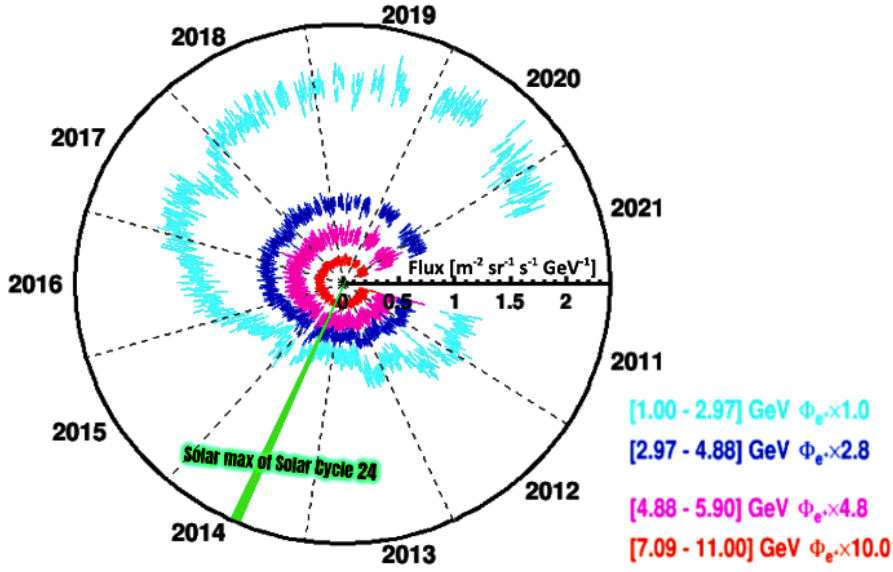
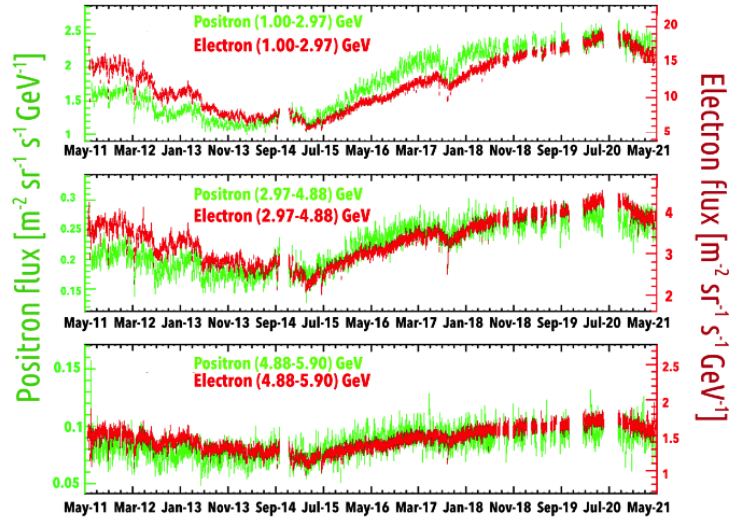


**Figure 2:** AMS 3-day positron fluxes,  $\phi_{e^+}$ , for four energy bins from 1.00 to 11.00 GeV, measured over the entire period. The scale of the fluxes are multiplied by different scale factors as indicated. As seen the positron flux exhibits variations at different timescales (short term variations and long term variations).

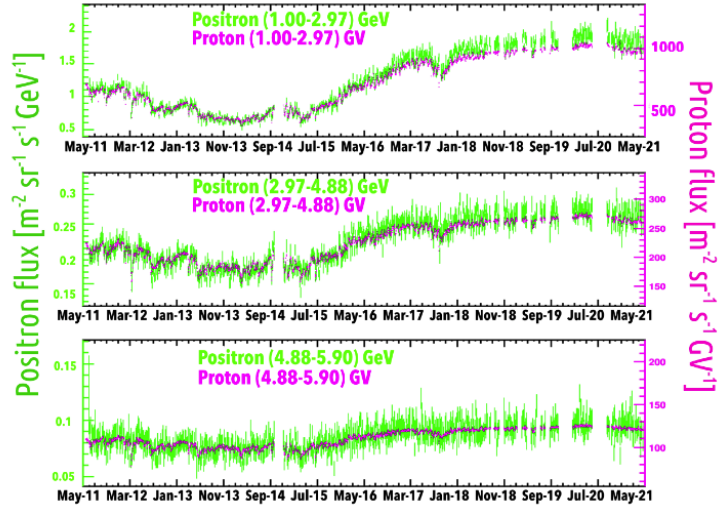
## 5. Solar polarity reversal effect - Long term variations

Simultaneous measurements of positron and electron fluxes over a complete solar cycle represent a unique test of the charge-sign dependencies in modulation models. On the other hand, simultaneous measurements of positron and proton fluxes [4], in the same period can provide a unique test of the mass dependencies in modulation models. The comparison of the long-term evolution of positron and electron fluxes is shown in figure 3a in three energy bins from 1.00 to 5.90 GeV for the ten-year period. As seen, from 2011 to 2014, the positron flux decreased slower with time than the electron flux, this trend changed from 2015 to the middle of 2017 when the positron flux rose faster, and finally, from the middle of 2020 to 2021, again decreased slower. This effect is clearly visible for the first energy bin and decreases with increasing energy. Therefore, a different behaviour before and after solar polarity reversal is observed for particles with the same mass and different charges. Figure 3b shows the positron and the proton flux for the same three energy bins and time period. A similar behaviour before and after solar polarity reversal is observed for particles with the same charge and different mass.

In addition, to investigate the difference in the modulation, comparisons using different moving averages, as indicated, are presented in figure 4. The data points correspond to fluxes averaged over 3 days for positron. Moreover, as seen in the top panel, a complex correlation between  $\phi_{e^+}$  and  $\phi_{e^-}$  is clearly observed, whereas a linear correlation is observed in the bottom panel between positron and proton fluxes.



(a) Positron Flux vs Electron Flux



(b) Positron Flux vs Proton Flux

**Figure 3:** 3-day positron fluxes (green points) together with (a) electron fluxes (red points) (b) proton fluxes (pink points) measured over the 10 years period for three energy (for electrons and positrons) or rigidity (for protons) bins from 1.00 to 5.90 GeV.

## 6. Solar Modulation Charge-Sign and Mass dependencies - Short term variations

To study the variability of the positron flux, the comparison of the short-term evolution with electrons and protons is carried out. Figure 5a shows the short-term variations of 3-day positron and electron fluxes (top panel) or proton flux (bottom panel) in the energy range from 1.00 to 2.97 GeV, during a time period in which solar polarity is negative and the positron flux exhibits non-recurrent time variations (from June 2011 to June 2012). As seen, the positron flux variations are different from those observed in the electron flux, whereas for protons are similar. In this case,

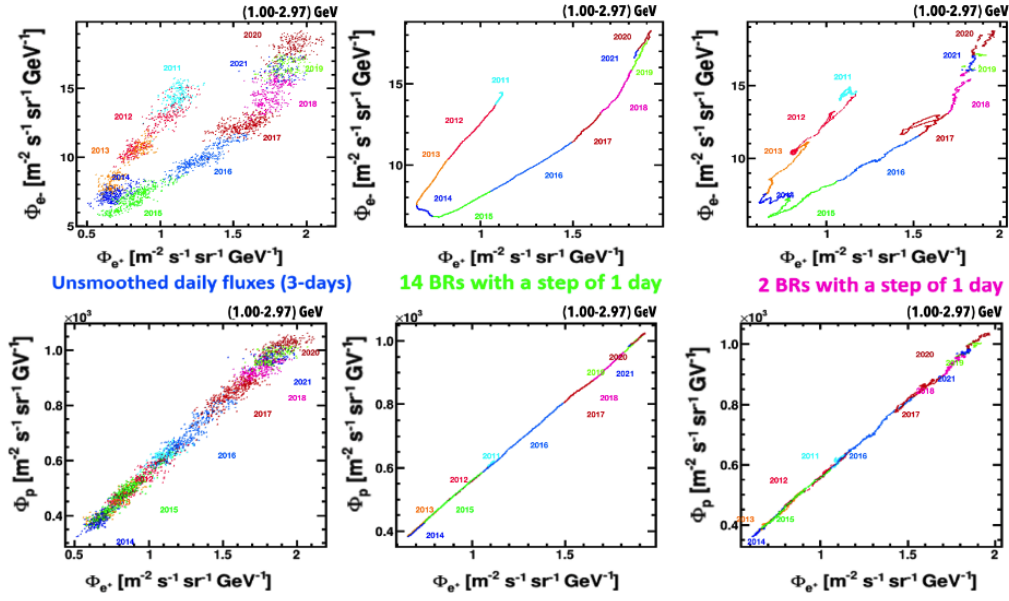
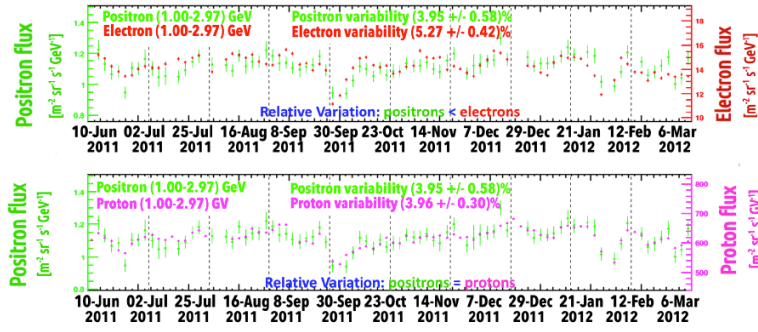


**Figure 4:** Top panel: Positron flux,  $\phi_{e^+}$ , versus electron flux,  $\phi_{e^-}$ , in the energy range 1.00 to 2.97 GeV. Bottom panel: Positron flux,  $\phi_{e^+}$ , versus proton flux,  $\phi_p$ , in the same energy interval. For positron flux, data points correspond to fluxes averaged over 3 days. The fluxes are calculated used different moving average as indicated. Different color indicate different years.

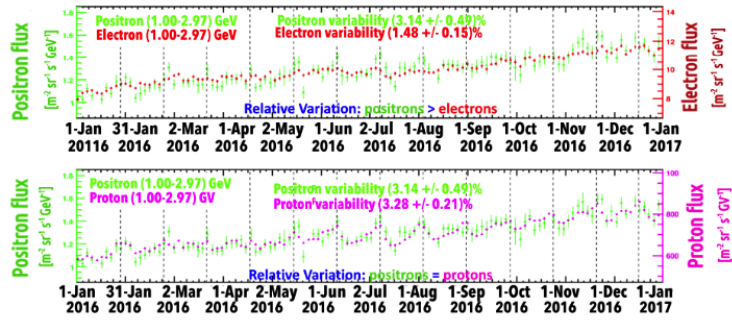
the positron variability is less than in electron flux. On the other hand, in figure 5b is shown the same fluxes but now during a time period which has positive solar polarity and the positron flux presents recurrent time variations (from January 2016 to January 2017). As seen, positron and proton fluxes exhibit similar behaviour during the entire period, whereas the positron flux exhibit more variability than the electron flux.

## 7. Conclusions

The charge-sign and mass dependent modulation during a complete solar cycle for daily positron flux has been investigated in detail. At long-term scale, distinct behaviour between positron flux and electron flux before and after solar polarity reversal are observed. At short-term scale, there are two scenarios; for particles with the same mass and different charge sign the time variability is different, while for particles with same charge and different mass the time variability is similar. On the other hand, complex correlations between positron and electron fluxes are observed, whereas positron and proton exhibit linear behaviour. AMS has already observed many interesting phenomena in the time evolution for the positron fluxes covering part of the solar cycle 24 and the beginning of the solar cycle 25, and will continue taking data until the end of the ISS operation (2030) allowing to extend these studies to the complete solar cycle 25.



(a) 2011, Solar polarity A&lt;0



(b) 2016, Solar polarity A&gt;0

**Figure 5:** (a) 3-day positron flux (green points), and 3-day electron flux (red points) or 3-day proton flux (pink points) in the energy range 1.00 to 2.97 GeV, measured from (a) June 2011 to June 2012, when solar polarity is negative, (b) January 2016 to January 2017, when solar polarity is positive. The positron flux exhibits recurrent and non-recurrent time variations which are similar in proton but different from those observed in the electron flux.

## References

- [1] M. Aguilar, et al. [AMS Collaboration], First Result from the Alpha Magnetic Spectrometer on the International Space Station: Precision Measurement of the Positron Fraction in Primary Cosmic Rays of 0.5-350 GeV. *Phys.Rev.Lett.* **110** 141102. (2013)
- [2] M. Aguilar, et al. [AMS Collaboration], The Alpha Magnetic Spectrometer (AMS) on the International Space Station: Part II - Results from the first seven years. *Physics Reports.* (2020)
- [3] M. Aguilar, et al. [AMS Collaboration], Towards Understanding the Origin of Cosmic-Ray Positrons. *Phys. Rev. Lett.* **122**, 041102 (2019)
- [4] M. Aguilar, et al. [AMS collaboration] Periodicities in the Daily Proton Fluxes from 2011 to 2019 Measured by the Alpha Magnetic Spectrometer on the International Space Station from 1 to 100 GV. *Phys. Rev. Lett.* **127**, 271102 (2021,12)